Collapsing Flow Topology Using Area Metrics

Wim de Leeuw, Robert van Liere
Center for Mathematics and Computer Science CWI,
Kruislaan 413, 1090 GB Amsterdam, Netherlands

Abstract

The technique for visualizing topological information in fluid flows is well known. However, when applied to turbulent flows, the result will be a cluttered image which is difficult to interpret. This paper presents a technique for collapsing topologies. The governing idea is to classify the importance of the critical points in the topology. By only displaying the more important critical points, a simplified depiction of the topology can be provided. Flow consistency is maintaining when collapsing the topology, resulting in a visualization which is consistent with the original topology. We apply the collapsing topology technique to a turbulent flow field.

Keywords: multi-level visualization techniques, flow visualization, flow topology

1 Introduction.

Helman and Hesselink introduced a technique for the visualization of vector field topology in fluid flows, [1]. Flow topology combines the simplicity of schematic depictions with the quantitative accuracy of curves computed directly from the data. Topology visualization captures the essential features when applied to simple flow fields. For more complex flows, however, the large number of critical points results in a difficult to interpret image. For example, consider the topology of a turbulent flow in figure 1. The data set is from a direct numerical simulation of flow around a square cylinder at a high Reynolds number. The image shows the topology of the skinfriction on one side of the cylinder. Small colored icons are used to display the set of critical points: a spiral icon denotes a focus, a blue cross denotes a saddle point, and disks denote nodes. Green is used to denote source points while red is used to denote sink points. Black trajectories are used to link critical points. The computed set of 338 critical points is very large. It is difficulty to perceive the global structure of the field due to cluttering of critical points and trajectories in the image. Note that critical points tend to be clustered in small local regions of the flow.

An approach to overcome the problem of cluttering would be to visualize a selection of the topology of the flow. The governing idea is to classify the importance of the critical points. By only displaying the more important critical points, a simplified depiction of the topology can be given, yet maintaining the global nature of the flow field.

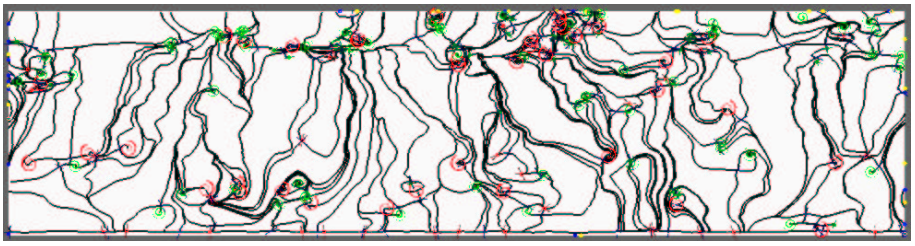

Figure 1: Skin friction on a square cylinder. The flow direction is from top to bottom. Critical points are shown as small colored icons and trajectories linking critical points are shown in red.

In a previous paper, [2], we proposed a technique for the visualization of global flow structures using multiple levels of topology. A filter mechanism was introduced that prunes less important critical points and visualizes only the remaining critical points. The filter is based on a user controlled distance metric between certain pairs of critical points. In this paper, we first generalize the notion of multiple level topology visualization. Second, a new method is introduced for maintaining topology consistency when deleting critical points. Third, a new filtering criterion based on an area metric, is introduced. The area metric is a more accurate classifier of the importance of critical points. The technique can be used to improve the importance in the selection of the set of critical points. The resulting visualization is simpler, yet consistent with the original topology.

The format of this paper is: In the next section we briefly review previous work. Section 3 introduces some nomenclature, discusses the notions of inflow and outflow areas and show how a topology can be collapsed without compromising topology consistency. In section 4, we discuss the computational aspects involved in constructing a topology graph and the steps involved in collapsing topologies. Finally, in section 5 we apply the technique to a complex application: the visualization of skin friction on a square cylinder in a turbulent flow field.

2 Related work

The visualization of vector field topology has been introduced by Helman and Hesselink, [1]. It presents essential information of a flow field by partitioning it in regions using critical points. Critical points are points in the flow where the velocity magnitude is equal to zero. Each critical point is classified based on the behavior of the flow field in the neighborhood of the point. For this classification the velocity gradient tensor is used. The velocity gradient tensor – or Jacobian – is defined as

$$\mathbf{J} = \nabla \vec{u} = \begin{pmatrix} u_x & u_y \\ v_x & v_y \end{pmatrix} \tag{1}$$

in which subscripts denote partial derivatives. The classification is based on the two complex eigenvalues ($R1 \; + \; i \; I1, \; R2 \; + \; i \; I2$). Assuming that the the critical point

is hyperbolic, i.e. the real part of the eigenvalues is non zero, five different cases are distinguished (see figure 2) : *Saddle point*, the imaginary parts are zero and the real parts have opposite signs; i.e $R1 * R2 < 0$ and $I1\ ,\ I2 = 0$. *Repelling node*, imaginary parts are zero and the real parts are both positive; i.e $R1\ ,\ R2 > 0$ and $I1,\ I2 = 0$. *Attracting node*, imaginary parts are zero and the real parts are both negative; i.e $R1\ ,\ R2 < 0$ and $I1,\ I2 = 0$. *Repelling focus*, imaginary parts are non zero and the real parts are positive; i.e $R1\ ,\ R2 > 0$ and $I1,\ I2 \neq 0$. *Attracting focus*, imaginary parts are non zero and the real parts are negative; i.e $R1\ ,\ R2 > 0$ and $I1,\ I2 \neq 0$.

When the real part of the eigen values is zero, the type of the flow is determined by higher order terms of the approximation of the flow in the neighborhood of the critical point.

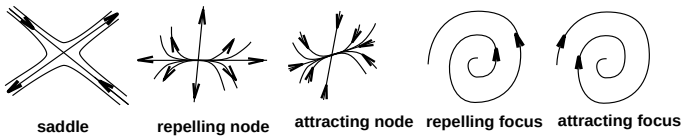

Figure 2: Five different types of critical points.

Trajectories traced from critical points in the direction of the eigenvectors of the velocity gradient tensor will partition the flow field in distinct regions.

In a previous paper, we have proposed a technique for the visualization of multiple levels of flow topology,[2]. A *pair distance filter* was introduced which prunes the set of all critical points. The motivation of this filter is that an often occurring small disturbance of the flow is caused by pairs of critical points. For example, the topological structure of a two dimensional vortex consists of a focus (repelling or attracting) or a center combined with a saddle point (see figure 3). The size of the vortex is determined by the distance between the pair of critical points. Removing the pair from the topology will result in a collapsed topology in which the global structure of the flow is still intact.

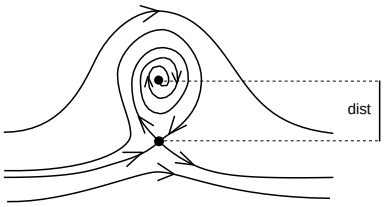

Figure 3: An example of a critical point pair; a focus and saddle point forming a vortex. The distance defines the spatial scale of the point pair.

Multi-level topologies is a first step to make flow topology analysis more useful for transient and turbulent flows. It has been successfully applied to a complex turbulent flow. Nevertheless, a number of drawbacks to the pair distance filter should be men-

tioned. First, the distance filter cannot be used to robustly determine the neighborhood relation near a number of critical points. For example, if there are three critical points all more or less with the same distance to each other, which pair is to be removed? Choosing the pair with the minimum distance is not always the correct choice. Second, the point deletion scheme does not take topology consistency into account. For example, deleting a critical point pair could result in a topology with two foci next to each other which both rotate in the same direction.

3 Concepts

In this section we introduce nomenclature of vector fields and flow functions and discuss the concepts of inflow and outflow areas. We illustrate these with a simple example. Refer to Asimov's notes on flow topology, [3], or Arnold's book on ordinary differential equations, [4], for a more rigorous treatment of these concepts.

Nomenclature We consider a flow field in $\Re^2$. Define $D \subset \Re^2$ as an closed set of Euclidean space $\Re^2$ bounded by a closed curve B.

The two dimensional *vector field* on D is given by a function $f : D \to \Re^2$. The *flow function* $\phi : D \times T \to D$ defines the trajectory of a point $p \in D$ for a time $t \in T$. In this paper, we assume that the topology of the flow field is continuous and is structurally stable; i.e. the topology will not change by an arbitrary small perturbation of ϕ.

Critical points are points p for which $\phi(p, t) = p$. We denote a *sink point* as p^{in} in which $p^{in} \in D$, a *source point* as $p^{out} \in D$, and a *saddle point* as $p^x \in D$.

The function $b : B \times \phi \to \Re$ as the mapping of every point on the boundary to $[-180.0,\ 180.0]$, depending on the angle of the tangent of ϕ with respect to the boundary B. A *boundary inflow*, denoted as B^{in} in which $B^{in} \subset B$, is defined as the curve segment for which the function b is positive. A *boundary outflow*, denoted as B^{out}, is defined as the segment for which the function b is negative. The points where $b = 0$ or $b = 180$ are called *switch points*. [1] We distinguish two types: A *positive boundary switch point*, denoted as p^{w+} in which $p^{w+} \in B$, is a point on the boundary in which ϕ points into B^{in}. A *negative boundary switch point*, denoted as p^{w-}, is a point on the boundary in which ϕ points out of B^{out}. Figure 4 illustrates the two possible cases.

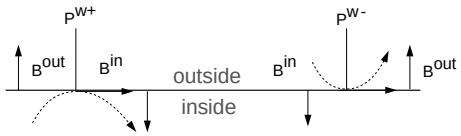

Figure 4: Boundary switch points are points on the boundary in which the tangent to the flow changes signs.

[1] This definition does not take into account the case that $b = 0$ along a segment of boundary B. It can be shown that these segments can be treated as switch points.

Flow Consistency The requirements of flow consistency are based on the notion of an *index*. The index of a closed curve in a vector field is defined as the number of revolutions made by the field vector in traversing the curve once.

The index of a critical point is defined as the index of a closed curve around the critical point which does not enclose any other critical point. Source and sink points have an index of 1. Saddle points have an index of -1.

Figure 5 illustrates indices of critical points and curves. Thin lines denote the flow function, while short thick arrows show the direction of the flow at the curve. The curve on the left has an index of 0, the source point has an index of 1 (middle), and the saddle point has an index of -1 (right).

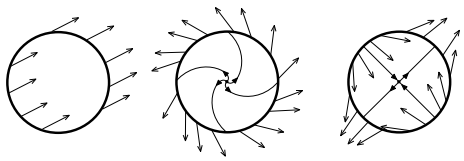

Figure 5: Indices of a curve containing zero critical points (index = 0), one source (index = 1), and one saddle (index = -1) point.

We denote the index of critical point p as $I(p)$ and the index of curve X as $I(X)$. A vector field is said to have a consistent topology if the following – necessary but not sufficient – condition is satisfied:

$$\sum_i I(p_i) \;=\; I(B) \tag{2}$$

in which p_i is a critical point and B is the boundary of D; i.e. sum of all critical point indices is equal to the index of the domain boundary. The index of boundary B is related to the number of boundary switch points by the equation:

$$I(B) \;=\; \frac{\#p^{w+} \;-\; \#p^{w-} \;+\; 2}{2} \tag{3}$$

in which $\#p^{w+}$ and $\#p^{w-}$ are resp. the number of positive and negative switch points.

Flow Regions Define a *sink region* as the set of points whose trajectories "end up in" a sink point p^{in}; i.e.

$$R^{p^{in}} \;=\; \{p \mid \lim_{t\to\infty} \phi(p,t) \;=\; p^{in}\} \tag{4}$$

in which $p^{in} \in D$ and p^{in} is a sink.

Similarly, a *source region* is the set of points whose trajectories "originate from" a source point p^{out}; i.e.

$$R^{p^{out}} \;=\; \{p \mid \lim_{t\to-\infty} \phi(p,t) \;=\; p^{out}\} \tag{5}$$

in which $p^{out} \in D$ and p^{out} is a source.

Define the *inflow region* as the set of points whose trajectories "enter" via boundary B^{in}; i.e.

$$R^{B^{in}} \;=\; \{p \mid \exists b \in B^{in}\, \exists t < 0 \;:\; \phi(p,t) \;=\; b\} \tag{6}$$

in which $B^{in} \subset B$ and B^{in} is an inflow boundary.

Similarly, an *outflow region* is the set of points whose trajectories "exit" via boundary B^{out}; i.e.

$$R^{B^{out}} \;=\; \{p \mid \exists b \in B^{out}\, \exists t > 0 \;:\; \phi(p,t) \;=\; b\} \tag{7}$$

in which $B^{out} \subset B$ and B^{out} is an outflow boundary.
Three interesting properties hold for source and inflow regions:

1. The intersection of any source or inflow region is empty.
2. Boundary segments of a source region can be constructed by following a trajectory which originates at a saddle (the two trajectories in the direction of the eignvectors for which the eigenvalues are positive) or positive boundary switch point. A boundary segment will link saddle points with sink points or outflow boundaries.
3. The boundary of a source region is a curve consisting of a collection of boundary segments.
4. Every point in domain D belongs to a source / inflow region or to a boundary of a source / inflow region.

Similar properties also apply to sink and outflow regions.

Flow areas The *flow area* of a region R, denoted as A^R, is the area of a region. Areas can be sorted as:

$$0 \;<\; A^{R^1} \;<\; A^{R^2} \;....\; <\; A^{R^n} \tag{8}$$

with n being the total number of inflow, outflow, sink and source regions.

The influence of a source/sink on the global structure of the flow field is determined by the corresponding region; the smaller the region, the smaller the influence. The area metric assigns the importance of each source/sink point as proportional to the area of the corresponding region. Less important points correspond to small areas.

Collapsing To simplify the topology a collection of critical points is replaced by a single critical point. To maintain topological consistency critical points cannot be removed arbitrarily; instead constrained collapsing must be used.

Collapsing a arbitrary closed region C bounded by B^C of domain D (i.e. $C \subset D$), must satisfy the following two conditions: first, the index of B^C is equal to 1 and second, B^C contains no switch points. These conditions imply that the B^C is a single boundary in/outflow with respect to C. Such a closed region can be contracted to a single critical point without changing the topology outside C and maintaining the flow consistency condition given in equation 2. The type of the contraction point (a source

or sink) is determined by whether B^C is an boundary inflow or outflow. All trajectories intersecting B^C will be connected to the contraction point.

We describe two examples of topologies that can be collapsed into a single contraction point (see figure 6). The first example (left) is where two sources are connected via a saddle. The three critical points are collapsed into a single source. In this case the closed region is an infinitesimal region around the three points and their connecting trajectories. In structurally stable fields a region satisfying the conditions needed for collapsing can always be found.

The second example (right) is a source region contraction. In this case, the closed region C is a complete source region and its boundary plus an infinitesimal layer around it. Collapsing results in a sink point. All trajectories linked to the sink points on the boundary will be connected to the sink point.

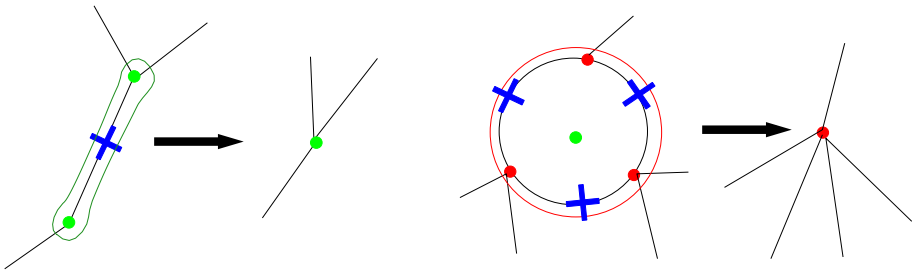

Figure 6: Two examples of topology collapsing. The left image collapse two sources and a saddle to a source point. The right image collapse a source region and its boundary to a single sink point.

Example Figure 7 illustrates these concepts. The left image shows the topology of a flow field containing 3 saddle (crosses) , 2 sink points (dots with directed incoming links), 1 source points (dots with outgoing links), and 6 boundary switch (points on boundary) points. Directed solid lines are drawn to link critical points. Directed dashed lines used to show lines that intersect with positive boundary switch points.

The middle image shows the shows the corresponding sink and outflow regions. Sink points are shown as six small incoming arrows. Outflow boundary regions are shown with a thick line and an outgoing arrow.

The right image shows the shows the source and inflow regions. Source points are shown as six small outgoing arrows. Inflow boundary regions are shown with a thick line and an incoming arrow.

4 Computational Model

In this section we discuss how to compute a collapsed topology based on an area metric. The algorithm consists of the following steps:

1. Construct the topology graph and compute the flow regions.

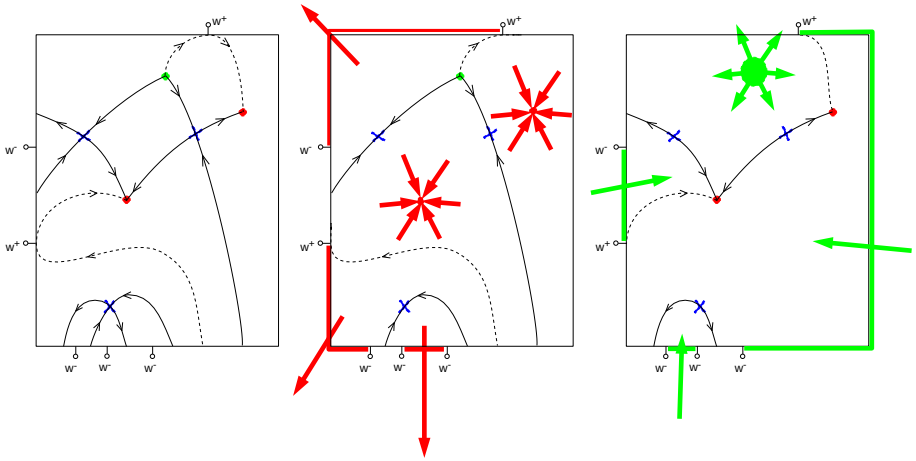

Figure 7: Example topology with corresponding sink/outflow regions (middle) and source/inflow regions (right).

2. Compute the area of each region.

3. Iteratively collapse regions until all remaining areas are greater than a user provided area threshold value. The source/sink/inflow/outflow region with the smallest flow area is collapsed first, followed by the region with the second smallest flow area, etc.

4. Draw the collapsed topology.

Steps 1 and 3 are detailed in the following sections.

4.1 Compute flow regions

We limit the discussion to source regions. Computing and collapsing sink regions are very similar. The two step procedure is outlined as:

1. construct topology graph

   For every saddle point in the data set D, trace two trajectories in the direction of the eigenvectors for which the eigenvalues are $\lambda > 0$; i.e. in the outgoing direction. These trajectories must end in a sink point or intersect the domain boundary at a boundary outflow. For every positive boundary switch point on the boundary of the data set, trace a trajectory in the outgoing direction of the switch point.

   Use the obtained information to construct a list of incoming trajectories for each sink point and boundary outflow. At each sink point this list is sorted as follows: Choose the first trajectory in the list. For all other trajectories at the source point compute the angle of the tangent vector of the trajectory with the tangent vector of the first trajectory; i.e. $angle(v_0, v_i) = \alpha_i$ where v_i is the tangent vector of trajectory s_i at the source point. Sort the list of trajectories in counterclockwise

order according to value of α_i (see figure 8). At each boundary outflow, the list of trajectories is sorted as follows: sort the intersections of the trajectories with the boundary counterclockwise along the boundary (see figure 8).

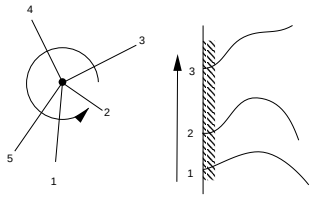

Figure 8: Counterclockwise sorting order of incoming trajectories at sink points and outflow boundaries. Trajectories are labeled according to their sorting order.

Similarly, for each source point and boundary inflow, construct a sorted list of outgoing trajectories.

2. compute region boundaries

   From each source point, choose an arbitrary trajectory from its sorted list. The end point of this trajectory (a saddle or a boundary) is labeled the starting point of the source region boundary. Assuming the starting point is a saddle, compute the two angles of the tangent vector of the incoming trajectory with the tangent vectors of both trajectories in the outgoing direction. Follow the trajectory with the smallest angle to a sink point or boundary outflow.

   Continue by choosing the next trajectory in the sorted list of trajectories associated to the sink point or boundary outflow. At a saddle point, continue by choosing the other trajectory associated with the same eigenvalue. Continue this procedure until the boundary ends in the starting point.

The idea of constructing a source region boundary is illustrated in figure 9. The left image shows a sample topology containing 7 saddle, 4 source and 4 sink points. Stippled lines denote sink/inflow regions and solid lines denote source/outflow regions. The middle image shows a zoomed in view of a source region consisting of a source point, 3 saddle and 3 sink points. Small diamonds are used to denote saddle points that are linked to the boundary. Trajectories originating from the source (shown in stippled lines) are labeled as $s_0,\ s_1,\ s_2$. Trajectories ending a sink point are labeled as $s_3,\ s_4,\ s_5,\ s_6$. Constructing the topology graph will result in a data structure shown on the right. For each point, the trajectories are sorted in counterclockwise order with respect to the angle of their tangent vector in the neighborhood of the point. To compute the region boundary, arbitrary choose and follow s_0 to the starting saddle point. Choose the outgoing trajectory with the smallest angle, i.e. s_4, and follow this trajectory to a sink point. Choose the next trajectory in the counterclockwise sorted list, i.e. s_6. Continue this procedure until the starting saddle point is reached.

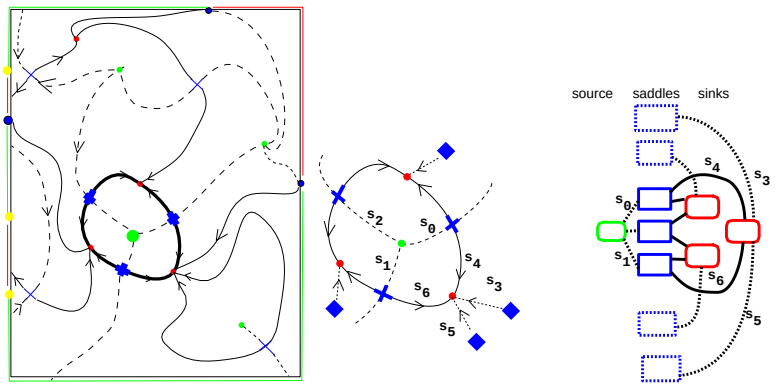

Figure 9: A sample topology (left) containing 7 saddle, 4 source and 4 sink points. Stippled lines denote sink/inflow regions, solid lines denote source/outflow regions. The detailed view is given of one source region (middle) with corresponding flow topology graph (right). The topology graph is used to construct the region boundary of the source region.

4.2 Collapsing Regions

We now discuss some implementation details of collapsing a source region into a single sink contraction point. The sink point on the boundary of the source region with the largest flow area is used as the contraction point. To prevent deformation of the domain boundary, a special case is used for region boundaries that contain a boundary outflow: in this case the boundary outflow is used as the contraction point. [2]

The idea of collapsing a source region is illustrated in figure 10. The left image show show the source region that is to be collapsed. Incoming trajectories to sink points on the boundary of the source region are joined to the contraction point by appending the already existing trajectory segments of the boundary. The middle image shows the collapsed topology graph. The right image shows the collapsed topology (stippled lines denote sink/inflow regions and solid lines denote source/outflow regions).

The region collapsing procedure maintains flow consistency, as defined by the relation $\sum_i I(p_i) = I(B)$; i.e. 1 source point, N saddle points and N sink points are replaced by 1 sink point. Hence, if the topology of the original data set is consistent, then the subsequent collapsed topologies will be consistent.

The motivation of reusing existing trajectory segments to reconstruct the topology graph is based on our desire that the collapsed topology closely resembles the original data.

4.3 Computational Errors

The collapsing topology technique described in the previous section works well in theory. In practice, however, there are various of sources of computational errors which

[2] We do not collapse the (more complicated) cases in which the boundary of the source region contains more than one boundary outflow because this would introduce deformation of the boundary.

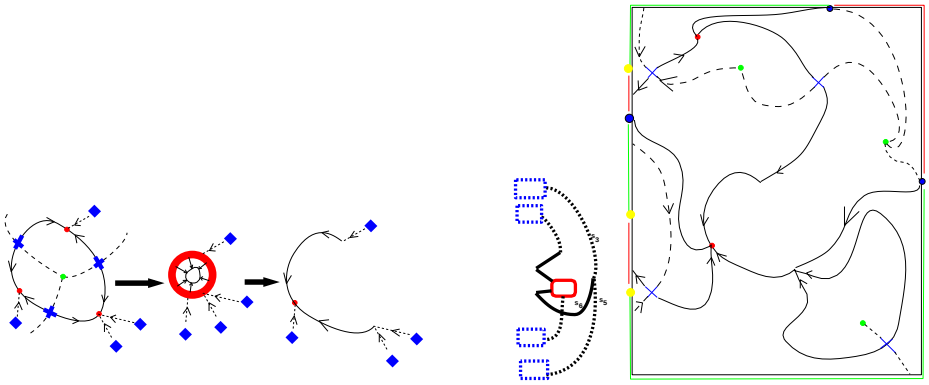

Figure 10: Collapsing a source region into a sink point (left). The source point and all critical points on the boundary of the region are replaced by one sink point and a collection of trajectories from the sink points on the boundary. The resulting topology graph is shown on the middle. On the right is the domain after collapsing the source region.

may lead to inaccurate results. We list a number of these errors:

- The step in which computational errors have the greatest consequences to the correctness of the technique is the trajectory integration. Computing trajectories is error prone due to the instability of the intergration process near critical points, [5]. In our implementation, even using an adaptive fourth order Runge-Kutta method, the integration was not stable. Stable adaptive integration has been addressed by reducing the time step when the angle of the computed segment with respect the the previous segment is too large.

- The distance criteria to stop integration when approaching a critical point is difficult to formulate. For example, in the case when two critical points are close together, the distance criteria must be sufficiently small. However, the the case when a trajectory approaches a rotation center, a small distance criteria may result in extremely long trajectories. In our implementation, we address this problem by extending the distance criteria with information on the type and eigenvectors of the critical point. For example, the stop distance is set to a larger value when approaching a rotation center.

- Computing the area of the a flow region may be error prone, due to the very large number of small segments that define a boundary. The impact this has on the technique is not very significant, only areas close to the threshold may be unjustly collapsed.

5 Skin Friction on a Square Cylinder

In [6], methods are discussed for direct numerical simulation (DNS) of turbulent flow. In this particular problem, a DNS of a turbulent flow around a square cylinder at Re =

22,000 (at zero angle of attack) has been performed. The resolution of the rectilinear grid is 314x538x64; the grid was finest nearby the cylinder. The number of time steps saved on disk are 7500. The skinfriction on all sides of the cylinder has been computed, resulting in four 2D data sets with a resolution of 104x64.

Figure 11 shows three collapsed topologies of the original topology of the skinfriction in figure 1. The flow direction is from top to bottom. The number of critical points in the original data set is 338. An increasing area threshold has been used to generate the images. From top to bottom: in topologies with respectively 139, 59 and 26 critical points.

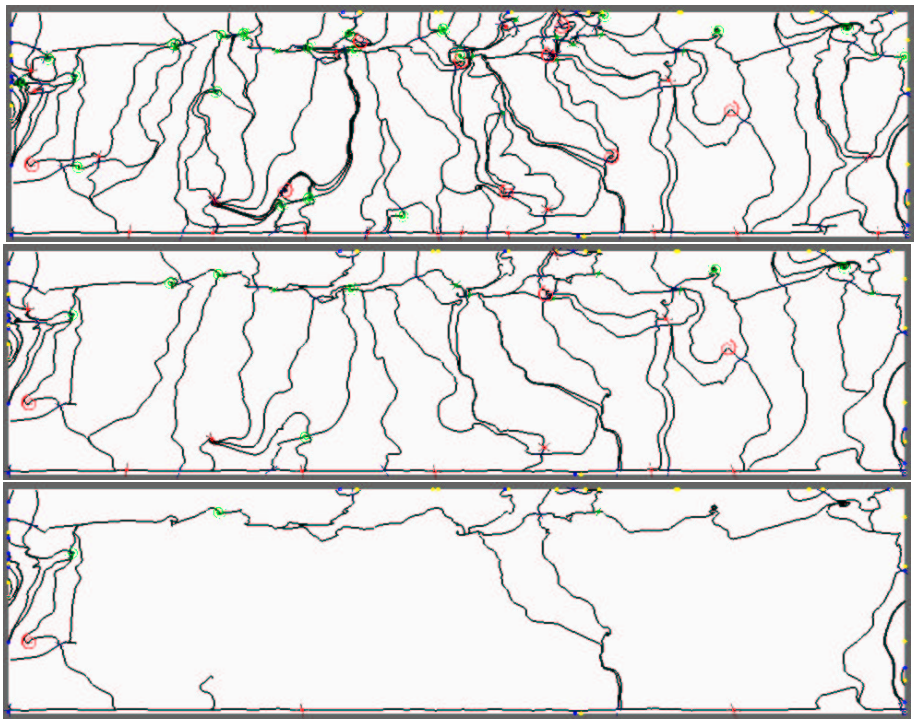

Figure 11: Collapsed topologies of skinfriction on a square cylinder with increasing area thresholds.

The skinfriction field on the square cylinder is characterized by two horizontal separation lines, located at the top and bottom of the image. The topological representation of the top separation line consists of a number of source and saddle points. The topological representation of the bottom separation line consists of a number of sink and saddle points. Trajectories originating from the saddle points link the saddles of the two lines.

The global structure of the is preserved using the area metric technique. The bottom image shows the most simplified view of the topology, yet the two main separation lines are preserved. The top image includes many important details caused by the turbulence of the flow. For this reason, the interactive threshold area metric is necessary to flip between images.

With regard to computational errors, the following should be observed: the cur-

rent implementation was not capable of computing the complete topology graph. The boundary of 5 (of total 167) source/sink regions could not completely be determined. This has probably been caused by trajectory intersections. The implementation assigns a very large area to these 5 regions. [3] Computation times for computing the initial topology graph (including trajectory computations) is in the order of 20 seconds on a 250 Mhz MIPS R10K processor. Determination of a collapsed topology for a threshold can be done in near real-time.

6 Conclusion

In this paper, a technique for the generation and visualization of collapsed topologies was presented. In this way a essential topological features of a flow field can be visualized without excessively cluttered image. The governing idea of the technique is to classify the importance of critical points. Critical point importance is related to its flow area which is determined by the topology graph. Consistency of the topology graph is maintaining when collapsing the topology. The collapsed topology closely resembles the original data.

After computing the topology graph, collapsing can be achieved in near real-time. This can be used to interactively vary the threshold area. For example, when zooming in on a part of the topology.

The technique has been applied to a complex turbulent flow data set from a direct numerical simulation. The application clearly benefit from the collapsed topology technique, [7]. The data set contain an abundance of detailed information. Using traditional topology visualization methods on these data sets, excessive cluttering can not be avoided. Using the collapsed topology based on area metrics technique, simplified views of the topology can be obtained without cluttering.

Acknowledgements

We wish to thank Prof. Arthur Veldman and Roel Verstappen of University of Groningen for sharing many ideas on very large flow data sets and providing the turbulent data sets. We also wish to thank Jack van Wijk of University of Eindhoven for many constructive comments when writing the paper.

References

[1] J.L. Helman and L. Hesselink. Visualizing vector field topology in fluid flows. *IEEE Computer Graphics and Applications*, 11(3):36–46, May 1991.

[2] W.C. de Leeuw and R. van Liere. Visualization of global flow structures using multiple levels of topology. In *Proceedings EUROGRAPHICS - IEEE TCCG Symposium on Visualization '99*, 1999. (to be published).

[3] Note to reviews: The images contain a number of regions close to the vertical boundaries that are not collapsed. This is caused by "bugs" in the current implementation which does not handle boundary in and outflows correctly in all cases. These bugs will be corrected in the final paper.

[3] D. Asimov. Notes on the topology of vector fields and flows. Technical Report Technical Report RNR-93-003, NASA Ames Research Center, 1993.

[4] V.I. Arnold. *Ordinary Differential Equations*. MIT Press, 1973.

[5] A. Globus, C. Levit, and T. Lasinski. A tool for visualizing the topology of three-dimensional vector fields. In G.M. Nielson and L.J. Rosenblum, editors, *Proceedings Visualization '91*, pages 33–40. IEEE Computer Society Press, Los Alamitos (CA), 1991.

[6] R.W.C.P. Verstappen and A.E.P. Veldman. Spectro-consistent discretization of navier-stokes: a challenge to RANS and LES. *Journal of Engineering Mathematics*, 34:163–179, 1998.

[7] A.E.P. Veldman. Private communication.